Trimethylsilyl Group Migration in the Mass Spectra of Trimethylsilyl Ethers of Cholesterol Oxidation Products. Product Ion Characterization by Linked-Scan Tandem Mass Spectrometry

Meg Annan, P. W. LeQuesne, and Paul Vouros
Department of Chemistry and Barnett Institute, Northeastern University, Boston, Massachusetts, USA

Loss of the A ring in the electron-impact mass spectra of the trimethylsilyl (TMS) derivatives of several cholesterol oxidation products is accompanied by intramolecular migration of the 3-O-TMS group to the charge-retaining portion of the molecule. Linked-scan techniques (B/E and B^2/E) were used to establish the fragmentation processes leading to the formation of the rearrangement ion. The TMS group appears to migrate to heteroatomic sites in the 5-, 6-, or 7-positions of the B ring. This structural assignment is supported by isotopic labeling studies and collision-induced dissociation of the resulting product ion. *(J Am Soc Mass Spectrom 1993, 4, 327–335)*

The trimethylsilyl (TMS) group has been extensively used for the derivatization of polar, thermally labile organic compounds owing to properties of the derivatives, such as reduced polarity, increased thermal stability, and simplification of mass spectral fragmentation modes [1]. In particular, the ease with which TMS ether derivatives are formed is due largely to the propensity of a silicon atom to form strong bonds with oxygen [2]. For instance, it was found that the trimethylsiliconium ion $(CH_3)_3Si^+$ readily forms adducts with compounds having oxygen-containing functional groups [3]. This behavior has motivated the use of $(CH_3)_3Si^+$ as a chemical ionization reagent. Much work has recently been done therefore with regard to the scope, mechanism, and energetics of tetramethylsilane chemical ionization [4–7]. Another facet of the tendency of silicon to interact strongly with oxygen is the tendency of TMS groups to migrate on electron-impact ionization of organic compounds. In fact, the migratory aptitude of the TMS group has been shown to be greater than that of hydrogen [8]. In addition, the TMS group has been shown to migrate over a wide range of distances as well as to a variety of electron-rich sites, including carbonyl and hydroxyl groups and carbon–carbon double bonds [9]. Of particular interest to us has been the observation of medium- and long-range TMS migrations in the electron-impact mass spectra of semirigid steroidal systems [10–12]. We have been interested in the development of a definitive gas chromatography/mass spectrometry (GC/MS) assay [13] for the analysis of cholesterol oxidation products, some of which are suspected of contributing to the formation of the arterial lesions and cell death associated with atherosclerosis [14, 15]. Recognition of these oxidation products and their origin is complicated by the susceptibility of cholesterol to undergo autoxidation in the presence of air and/or light, thus making commercially prepared foodstuffs containing dried eggs or dairy fat a potential source of angiotoxic substances. In the course of these GC/MS studies, we have become aware of the electron-impact-induced migration of a TMS group that initiates A-ring cleavage in the mass spectral fragmentation of cholesterol oxidation products. This fragmentation appears to be a variation of that reported by Brooks et al. [10]. Because TMS ether derivatives are important in the analysis of steroids by GC/MS, it is important to understand and recognize the rearrangement and fragmentations initiated by the TMS group. Such an understanding can then be of use in the characterization of unknown sterols. Toward this end, isotopic labeling and

Address reprint requests to Paul Vouros, Department of Chemistry and Barnett Institute, Northeastern University, Boston, MA 02115.

1044-0305/93/$6.00

Received August 24, 1992
Revised October 30, 1992
Accepted November 9, 1992

collision-induced dissociation (CID) of these derivatives were performed. The TMS derivatives of the cholesterol oxidation products studied are shown in Figure 1.

Experimental

Cholesterol Oxidation Products

Steroid standards were obtained from several sources. The cholestane-3β,5α,6β-triol was purchased from Research Plus Laboratories Inc. (Denville, NJ). The 5-cholestene-3β,25-diol; 3β-hydroxy-5-cholesten-7-one; 3β-hydroxy-5α-cholestan-6-one; 5,6α-epoxy-5α-cholestan-3β-ol; 5-cholestene-3β,7α-diol; and 5-cholestene-3β,7β-diol were purchased from Steraloids, Inc. (Wilton, NH). The 5,6β-epoxy-5β-cholestan-3β-ol was obtained from the College of Pharmacy, Northeastern University (Boston, MA). Selected standards were purified by reversed phase high-performance liquid chromatography as needed. TMS derivatives were prepared by dissolving 1 mg of analyte in 250 μL of silylation grade pyridine and 250 μL of *N*,0-bis(trimethylsiliyl)trifluoroacetamide (BSTFA) (both of Pierce Chemical Co., Rockford, IL). The samples were heated at 80 °C for 12–18 h. The pyridine and excess BSTFA were removed by evaporation by gentle heating under a stream of nitrogen. The samples were then redissolved in 1 mL of hexane. In the case of the triol, the 3,6-bis-TMS ether was the predominant product. The [$^2H_9$]-TMS derivatives were prepared in the same way except that 20 μL of [$^2H_{18}$]-*N*,0-bis(trimethylsilyl)acetamide (MSD Isotopes, St. Louis, MO) was used as the derivatization reagent. The [6 – ^{18}0]3β-hydroxy-5α-cholestan-6-one was produced by dissolving 1 mg of unlabeled material in 50 μL of a 2 mM HCl solution in isopropanol and 25 μL of H_2 ^{18}O (98%) (Cambridge Isotope Labs, Woburn, MA). The mixture was heated at 70 °C for 4 h, until the ^{18}O:^{16}O ratio was 2:1. The reaction was dried under gentle heating and a stream of nitrogen. The residue was then derivatized as described above.

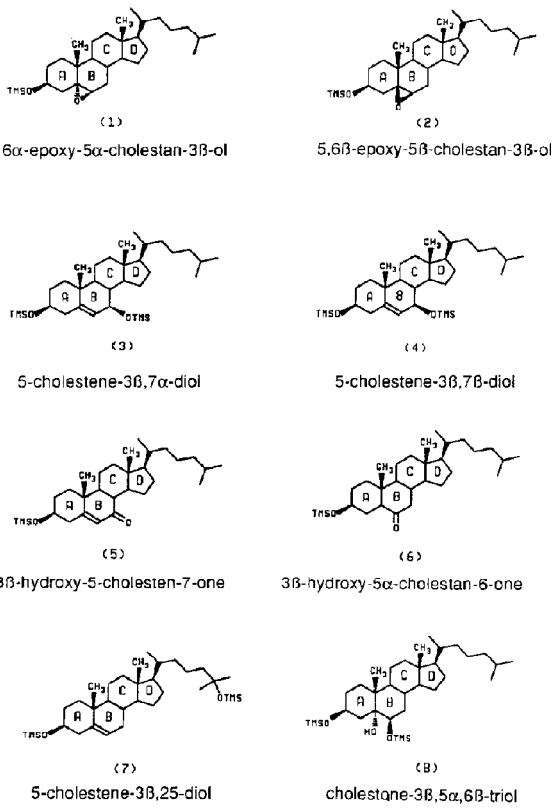

Figure 1. TMS derivatives of cholesterol oxidation products evaluated in this study.

Mass Spectrometry

All analyses were performed on a VG-70-250SE double-focusing mass spectrometer. Samples were introduced into the mass spectrometer via the heated solids probe. All experiments were done with the source operating at 180 °C, an electron energy of 70 eV, and an acceleration potential of 8 kV. Collision-induced dissociation experiments were done at 8 kV in a collision cell located in the first field-free region. The collision gas was He and was added so as to attenuate the precursor ion beam to 30%.

Results

Electron-Impact Mass Spectra

Common fragment ions observed in the electron-impact spectra of the compounds in Figure 1 are summarized in Table 1. The observed ions are typical of alicyclic TMS ethers. For example, as shown in Table 1, well-defined molecular ion peaks, followed most commonly by sequential neutral losses of $\cdot CH_3$, H_2O, CO, HCO$\cdot$, and trimethylsilanol (TMSiOH) are observed. The relative intensities and the combinations of these losses vary according to the structure of the parent oxidation product. The loss of TMSiOH is an important decomposition pathway because it is observed in all eight cases. Also prominent in the mass spectra of several of the compounds is the ion at m/z 129, which comprises C_1, C_2, and C_3 along with the trimethylsilyloxy function at C_3 (CH_2=CH–CH=O^+–TMS) [16]; however, the complementary fragment $[M - 129]^+$ is not generally observed.

Of particular relevance to this study is migration of the TMS group with concomitant cleavage of the A ring to yield an ion of m/z 403. This was observed in the spectra of all of the compounds in Figure 1 except for those of the 7- and 25-hydroxylated products. To confirm the presence of the TMS group on the charge-retaining fragment, the spectra of the corresponding [$^2H_9$]-TMS derivatives were also obtained. In each

Table 1. Common neutral losses in the electron-impact mass spectra of cholesterol oxidation products

Oxidation product[a]	Molecular ion (*m/z*)	Common ions, *m/z* units (neutral loss, u)
α-Epoxide (1)	474	459 (15), 456 (18), 445 (29), 403 (71), 384 (90), 369 (90 + 15), 366 (90 + 18), 356 (90 + 28)
β-Epoxide (2)	474	459 (15), 456 (18), 445 (29), 403 (71), 384 (90), 369 (90 + 15), 366 (90 + 18), 356 (90 + 28)
7α-Hydroxy (3)	546	531 (15), 456 (90), 367 (90 + 89), 366 (90 + 90), 351 (90 + 90 + 15), 253 (90 + 90 + 113), 129
7β-Hydroxy (4)	546	531 (15), 456 (90), 367 (90 + 89), 366 (90 + 90), 351 (90 + 90 + 15), 253 (90 + 90 + 113), 129
7-Keto (5)	472	457 (15), 455 (17), 444 (28), 429 (28 + 15), 416 (56), 403 (69), 382 (90), 367 (90 + 15), 269 (90 + 113), 129
6-Keto (6)	474	459 (15), 445 (29), 418 (56), 403 (71), 384 (90), 369 (90 + 15)
25-Hydroxy (7)	546	531 (15), 456 (90), 441 (90 + 15), 336 (90 + 90), 351 (90 + 90 + 15), 327 (90 + 129), 271 (90 + 129 + 56)
3β,5α,6β-Triol (8)	564	546 (18), 531 (18 + 15), 474 (90), 459 (90 + 15), 456 (90 + 18), 445 (90 + 29), 404 (90 + 70), 403 (90 + 71), 384 (90 + 90), 369 (90 + 90 + 15), 336 (90 + 90 + 18)

[a]Numbers in parentheses refer to compounds in Figure 1.

case, as shown in Table 2, the ion at *m/z* 403 is shifted by 9 u to *m/z* 412. In line with this, a plausible mechanism for the fragmentation of the epoxides (**1** and **2**), the 6-ketostanol (**6**) and the triol (**8**) is shown in Scheme Ia and b. Because the behavior of the α- and β-epoxides was found to be similar, they are collectively referred to as *the epoxide*. As shown in Scheme Ia, fragmentations are proposed for each derivative that lead to a common intermediate fragment ion (**9**). In each case, migration of the TMS groups is believed to be induced by the presence of a radical ion site at the heteroatom on the B ring. In the case of the triol, prior loss of TMSiOH is proposed to generate the same intermediate ion as that formed in step **b** by the epoxide. The remainder of the fragmentation process, starting with ion intermediate **9**, is shown in Scheme Ib. It is envisioned that subsequent cleavage of the A ring leads to the elimination of a stable neutral (71 u) and an ion at *m/z* 403. The structural commonality of this ion for the spectra of all four compounds is further supported by the CID data, as discussed below. In contrast to the spectra of compounds **1**, **2**, **6**, and **8**, the spectrum of the 7-ketosterol derivative (**5**) exhibits an ion at *m/z* 403 due to the loss of 69 instead of 71 u. This requires retention of two hydrogen atoms by the *m/z* 403 ion, presumably via a more involved rearrangement process. Consistent with the postulated transfer of the TMS group to an oxygen heteroatom, structures **11a** and **11b** in Scheme II are proposed for the resulting *m/z* 403 ion. Structures **11a** and **11b**

Table 2. Isotopic labeling experiments. Observed peaks and corresponding neutral losses, possibly resulting from TMS group migration.

Oxidation product[a]	Isotopically labeled analog, *m/z* (neutral loss, u)		
	Unlabeled	$^{2}H_{9}$-TMS	[6 $-^{18}O$]
α-Epoxide (1)	403 (−71)	412 (−71)	NA[b]
β-Epoxide (2)	403 (−71)	412 (−71)	NA
7-Keto (5)	403 (−69)	412 (−69)	NA
6-Keto (6)	403 (−71)	412 (−71)	405 (−71)
	305 (−56 − 113)	314 (−56 − 113)	307 (−56 − 71)
3β,5α,6β-Triol (8)	403 (−90 − 71)	412 (−99 − 71)	NA

[a]Numbers in parentheses refer to compounds in Figure 1.
[b]NA, not applicable.

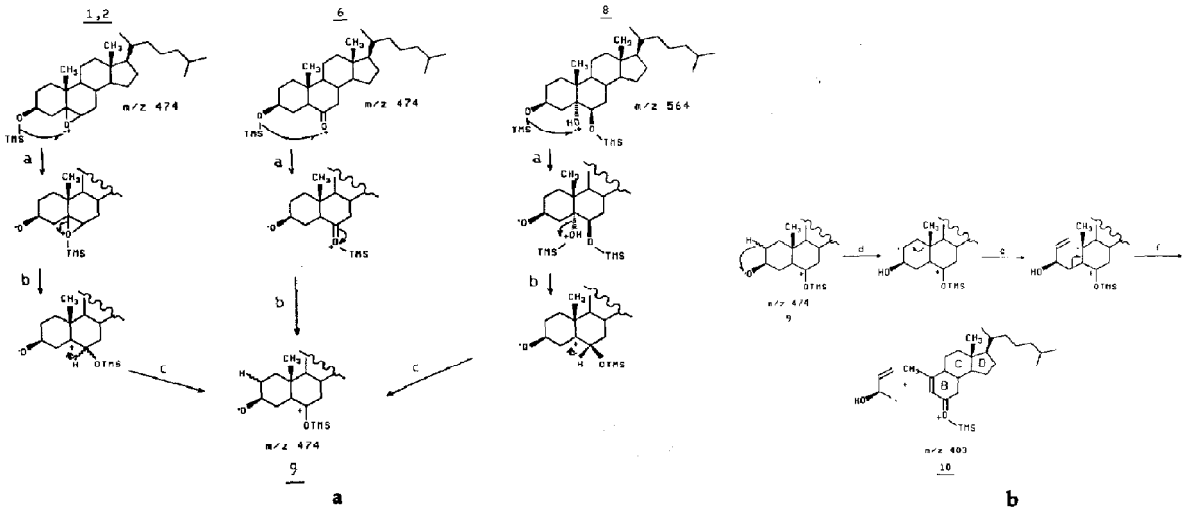

Scheme I. (a) Formation of a common intermediate in the electron-impact-induced TMS migration and A-ring cleavage of compounds **1**, **2**, **6**, and **8**. (b) Formation of the final ionic product at m/z 403 from the electron-impact-induced TMS migration in compounds **1**, **2**, **6**, and **8**.

differ from **10** in the position of the TMS oxonium function. In addition, **11a** differs from **10** and **11b** in that the TMS oxonium function is not conjugated with a carbon–carbon double bond.

In the mass spectrum of compound **6**, a possible rearrangement ion analogous to that of m/z 403 was also observed at m/z 305. This ion is effectively $[M - 56 - 113]^+$, the loss of 56 u being similar to that fragment reported by Brooks et al. [10]. The other neutral fragment lost corresponds to 113 u, the mass of the C_8H_{17} side chain. Two plausible mechanisms are outlined for this process in Scheme IIIa and b. In Scheme IIIa, the formation of intermediate ion **12** is shown, after which the mechanisms diverge as shown in Scheme IIIb. Path a involves a concerted loss of the A ring and side chain. Alternatively, path b is a stepwise process involving TMS migration and cleavage of the A ring at the C_1–C_{10} and C_3–C_4 bonds, as described by Brooks et al. [10], followed by the loss of the side chain. Finally, as shown in Table 2, the m/z 305 ion is shifted by 9 upon perdeuteration of the TMS group. The same ion is also shifted by 2 u in the spectrum of the [6 – ^{18}O]-labeled analog.

To substantiate the proposed mechanisms, it was important to establish relevant relationships between the key fragment and precursors. First, a direct precursor/product relationship must be established between the molecular ion, or $[M - TMSiOH]^+$ in the case of the triol, and the fragment ion of interest. Second, it must be demonstrated that the TMS group remains on the charge-retaining fragment and that it is bonded to the oxygen function on ring B. Finally, the proposed

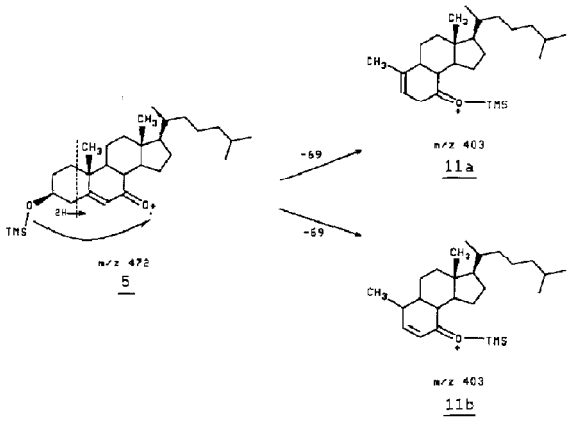

Scheme II. Proposed product of TMS migration and A-ring cleavage on electron-impact ionization of 3β-hydroxy-5-cholesten-7-one.

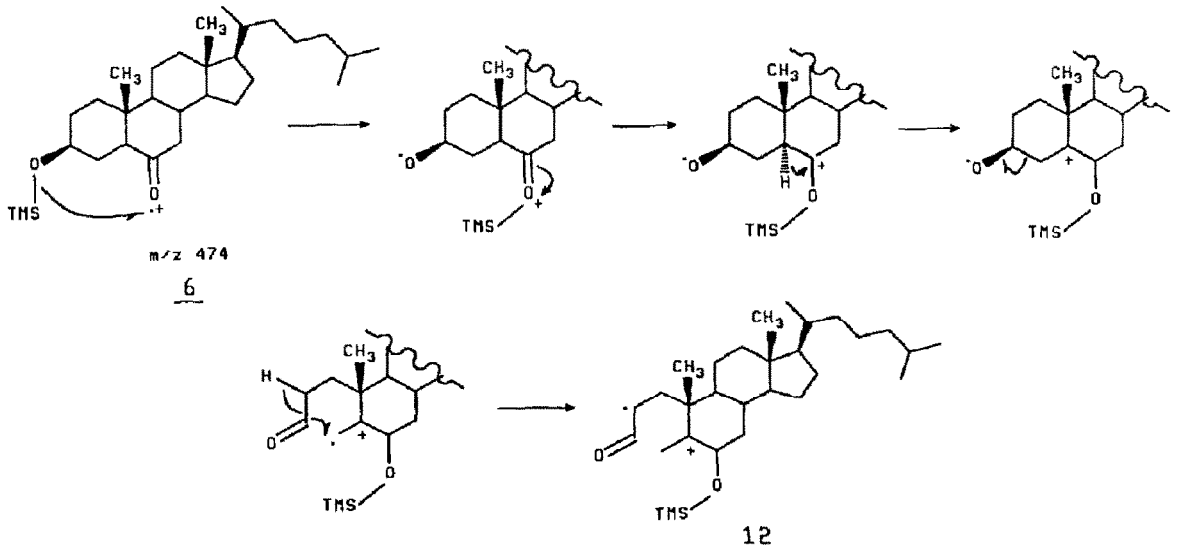

a

Scheme IIIa. TMS migration and C_3–C_4 bond cleavage in the electron-impact-induced formation of m/z 305 from 3β-hydroxy-5α-cholestan-6-one.

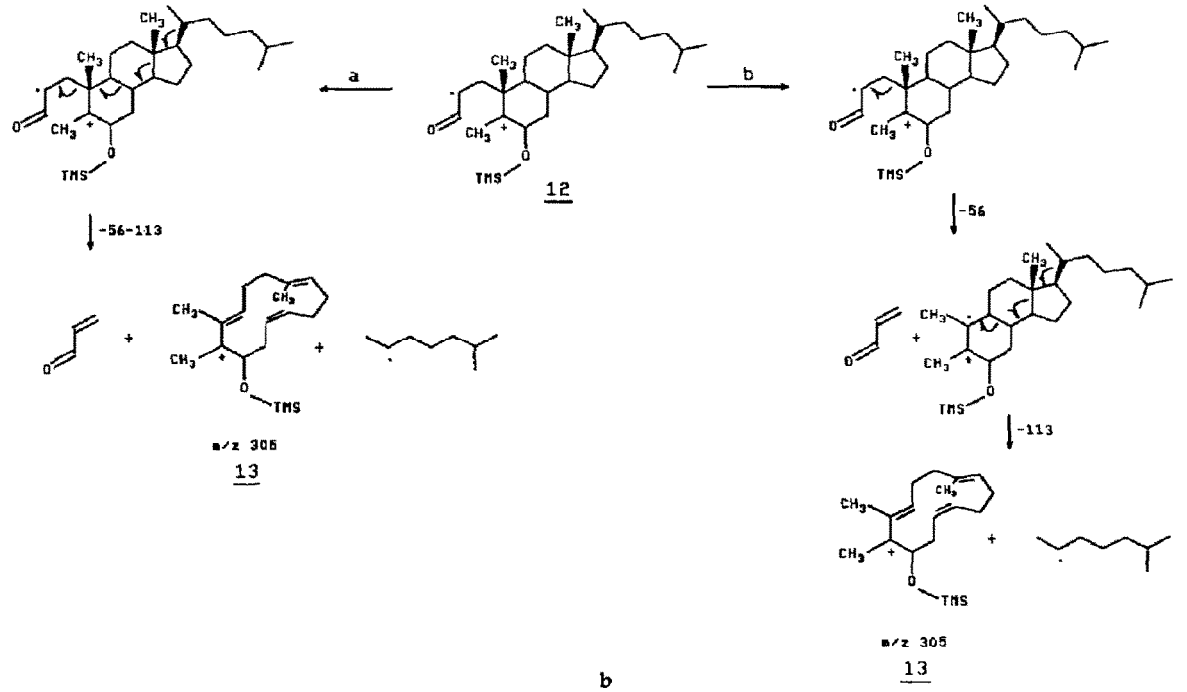

b

Scheme IIIb. Concerted or stepwise elimination of the A-ring and the C_8H_{17} side chain in the formation of m/z 305 from 3β-hydroxy-5α-cholestan-6-one.

ion structures must be consistent with the fragmentation patterns observed under collisional activation.

Metastable Analysis: B/E- and B^2/E Linked Scanning

The metastable decomposition spectra of the molecular ions from **1**, **5**, and **6** were obtained to confirm that m/z 403 was a direct product of the molecular ion. The results from B/E linked scanning demonstrate the appropriate precursor/product relationship in all cases, except for the $[M]^{+\cdot}$ to $[M - 56 - 113]^+$ transition proposed for the 6-ketostanol derivative in Scheme III. In the case of the triol, m/z 403 is thought to be preceded by formation of $[M - TMSiOH]^{+\cdot}$, m/z 474, which arises from TMS group migration to the 5α-hydroxyl group (Scheme Ia). Indeed, the metastable data in Table 3 confirm that the m/z 403 ion is derived from the m/z 474 fragment.

Although the metastable (B/E) data in Table 3 unequivocally link the m/z 403 ion to the indicated precursors, it was deemed important to also consider the genesis of this ion from the analogous $[M - 56]^{+\cdot}$ ion via the additional loss of a methyl group. Consideration of this alternative was necessary in light of the work done by Brooks et al. [10], who demonstrated a TMS migration in the formation of the ion $[M - 56]^{+\cdot}$ in the mass spectra of a wide range of trimethylsilylated Δ^5-hydroxysteroids. Linked scanning in the B^2/E mode was used for this purpose and yielded interesting additional information with regard to alternative pathways. These data support alternative pathways in the case of the epoxide, 6-ketostanol, and triol. For instance, precursor scans of m/z 403 in the case of the epoxide and the 6-ketostanol, indeed, show a strong metastable decomposition of the $[M - 56]^{+\cdot}$ intermediate ion at m/z 418 (see Table 3). A weak metastable decomposition directly linking the molecular ion m/z 474 to the m/z 403 fragment ion is also observed. These data support two competing pathways, one of which is a two-step fragmentation, the second step occurring in the time frame of metastable decompositions (Scheme IIIb), and a second single-step transition that presumably occurs within the time domain of ion source decompositions (Scheme IIIa). In the case of the triol, another precursor to the m/z 403 ion was found at m/z 546. This particular precursor ion arises via loss of H_2O from the molecular ion and apparently undergoes complete A-ring cleavage without prior TMS group migration. The resulting sequence of losses is presumably $[M - H_2O - 143]$. An exception again is the spectrum of the 7-ketosterol derivative (**5**). The presence of a single peak at m/z 474 in the B^2/E scan of m/z 403 from this particular derivative indicates only one precursor.

A direct precursor/product relationship between the molecular ion of the 6-ketostanol at m/z 474 and the ion at m/z 305 was not found by B/E linked scanning. Such a relationship was, however, observed under the B^2/E linking scanning mode. The predominant metastable decompositions leading to m/z 305 originate, however, from m/z 334 and 320. The pathway proceeding via m/z 334 is envisioned to be $[M - 140 - 29]$, the first loss possibly being attributed to cleavage through the C_{13}–C_{17} and C_{15}–C_{16} bonds of the D ring, followed by additional alkyl ($\cdot C_2H_5$) loss. The other intense precursor to m/z 305, the ion of m/z 320, is believed to arise via analogous cleavage through the C_{13}–C_{17} and C_{14}–C_{15} bonds of the D ring, followed by loss of $\cdot CH_3$. Again, B^2/E scans support other pathways that because of kinetic factors predominate in the metastable time regime. Most important, the B^2/E data indicate that the formation of m/z 305 is at least in part due to a concerted loss of the side chain and the A ring from the molecular ion. Furthermore, the B^2/E spectra also show that there is a window of approximately ±1% in the selection of the precursor ion. This is indicative of the parent selectivity in the B/E spectra, and therefore appropriate caution is warranted in the interpretation of such data.

Table 3. Metastable transitions observed using B/E- and B^2/E-linked scanning experiments

Oxidation product[a]	Transition (m/z)	Scan mode: B/E[b]	Scan mode: B^2/E[b]	Other precursors (m/z)
α-Epoxide (1)	474–403	+	+	418
β-Epoxide (2)				
7-Keto (5)	472–403	+	+	None
6-Keto (6)	474–403	+	+	418
	474–305	−	+	320, 334, others
3β,5α,6β-Triol (8)	474–403	+	+	546

[a]Numbers in parentheses refer to compounds in Figure 1.
[b](+) Observed via linked scanning; (−) not observed via linked scanning.

Collision-Induced Dissociation Using B/E Linked Scanning

A combination of isotopic labeling and CID was used next to address the second and third criteria mentioned above, namely, the proposed structural identity of m/z 403, the ion apparently produced from the TMS migration indicated in Schemes Ia, b, and II. On the basis of the mechanism proposed in Scheme Ib, a common ionic product is predicted in the formation of m/z 403 on ionization of the epoxide, the 6-ketostanol, and the triol. The resulting ion is expected to be highly stabilized by charge delocalization and the presence of a silicon atom beta to the cationic center [17]. The high-energy CID spectra of m/z 403 from these three precursors are shown in Figure 2. Significantly, these spectra are qualitatively similar, the major peaks being common to all three CID spectra. To determine which

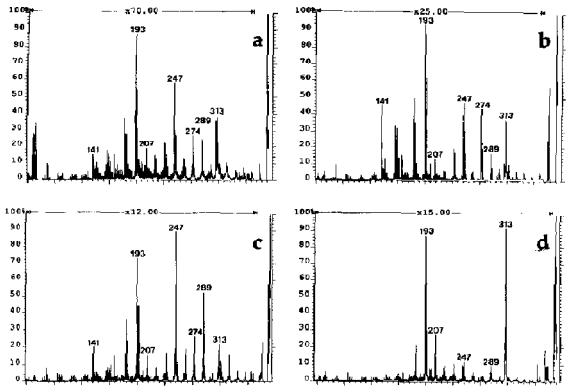

Figure 2. CID of m/z 403 from electron-impact ionization of (**a**) 5,6α-epoxy-5α-cholestan-3β-ol; (**b**) 3β-hydroxy-5α-cholestan-6-one; (**c**) cholestene-3β,5α,6β-triol; and (**d**) 3β-hydroxy-5-cholesten-7-one.

of the fragmentations in the CID spectra involve the loss of the TMS group or any segment thereof, CID of m/z 405 and 412, derived from the [6 $-{}^{18}$O]- and the [$^2H_9$]-TMS-labeled derivatives, was performed. As a representative example, the CID spectra of the $[M - 71]^+$ fragment ion from labeled and unlabeled analogs of 6-ketocholestanol can be compared in Table 4. Of the peaks indicated, three can be definitely associated with loss of the TMS group. The peak at m/z 313 can be attributed to the loss of TMSiOH on the basis of the absence of a mass shift in the CID spectrum of the [6 $-{}^{18}$O]- and the [$^2H_9$]-labeled derivatives. The same is true of the peak at m/z 274, which is not shifted on isotopic labeling. The origin of this peak is likely to be a result of B-ring cleavage, as shown in Scheme IV. In this case, an odd-electron ionic product and a neutral radical containing the TMS group are proposed. A further example of fragmentation associated with the B ring is the peak at m/z 141, which, based on its mass shift to 150 on perdeuteration of the TMS group, may be attributed to cleavage through the B ring at the C_6–C_7 and C_9–C_{10} bonds, also shown in Scheme IV. The other peaks in Table 4 are believed to result from loss of the side chain and various cleavages through

Table 4. Fragment ions observed on CID of m/z 403, 405, and 412 produced from labeled and unlabeled TMS derivatives of 3β-hydroxy-5α-cholestan-6-one

Unlabeled (m/z)	6 $-{}^{18}$O-labeled (m/z)	$^2H_9$-TMS-labeled (m/z)
313	313	313
289	291	298
274	274	274
247	249	256
207	209	216
193	195	202
141	NA[a]	150

[a] NA, not available.

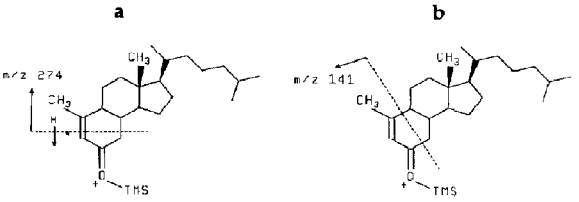

Scheme IV. Fragmentations involving B-ring cleavage in the CID spectra of m/z 403 derived from epoxide, triol, and 6-ketostanol derivatives.

the C and D rings. The major processes are indicated in Scheme V. As shown in Table 4, all four of these fragment ions exhibit the appropriate mass shift on isotopic labeling. The propensity for cleavages remote from the charge site is consistent with the proposed ion structure in which the charge on the B ring is stabilized via extensive delocalization.

Of particular significance is the consistent elimination of 90 u (TMSiOH) on CID of the m/z 403 ion from all four derivatives. This strongly suggests that the TMS group on the A ring does indeed become bonded to the oxygen function on the B ring. As shown in Table 2, the 9-u mass shifts of the m/z 403 ion in the spectra of each [$^2H_9$]-TMS derivative support the presence of the TMS group on the charge-retaining unit. Furthermore, the data in Table 4 indicate that the mass of the ion formed by loss of TMSiOH in the CID spectra of the isotopically labeled precursors is not shifted. Thus, the dual evidence of loss of both the [$^2H_9$]-TMS group and the [6 $-{}^{18}$O] atom in the collision-induced elimination of TMSiOH from labeled precursors is consistent with the formation of a Si–O bond during the TMS migration observed in the electron-impact spectra of these compounds.

As shown in Scheme II, two plausible structures (**11a** and **11b**) are proposed for the ionic fragment at

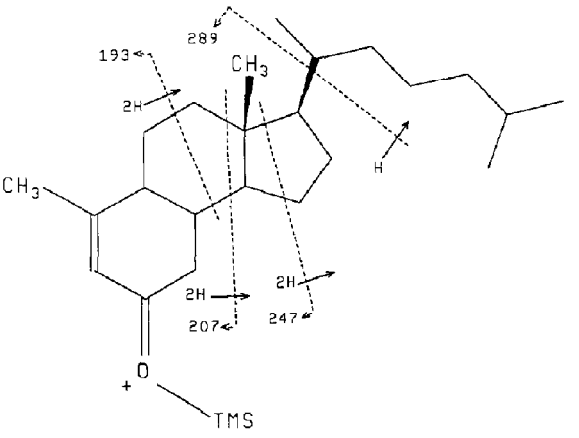

Scheme V. Charge-remote skeletal cleavage in the CID spectra of m/z 403 derived from epoxide, triol, and 6-ketostanol derivatives.

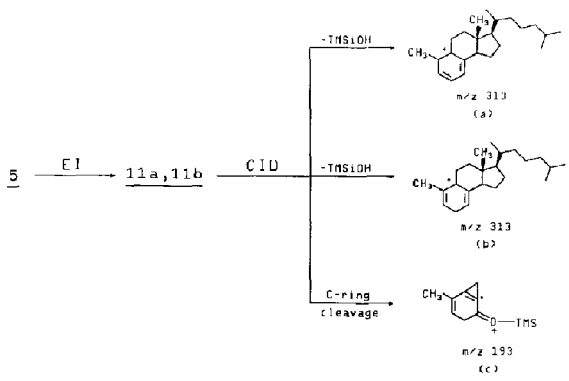

Scheme VI. CID of m/z 403 produced by electron-impact ionization of 3β-hydroxy-5-cholesten-7-one.

m/z 403 produced by fragmentation of the 7-ketosterol derivative. Both of these structures differ from the analogous ion produced by the epoxide, 6-ketostanol, and triol (**10**) in the position of the TMS oxonium function. The structure **11b**, however, is similar to **10** in that the TMS oxonium function is in conjugation with a carbon–carbon double bond. If the 7-ketosterol produces predominantly **11a**, the difference in charge stabilization is expected to affect the CID spectrum. This is in fact what is observed. As seen in Figure 2d, all but one of the charge-remote processes are suppressed. The two major peaks are at m/z 313 and 193, the former being due to loss of TMSiOH and the latter to cleavage through ring C. It is thus not surprising that the CID spectrum is dominated by these two processes because both can conceivably generate a more stable cation by extending the charge delocalization, as shown in Scheme VI.

The information obtained from the CID of m/z 305, $[M - 56 - 113]^+$, derived from the 6-ketostanol derivative was, however, less definitive. Comparison of the loss of TMSiOH in the unlabeled [$^2H_9$]-TMS- and [6 – ^{18}O]-labeled fragments does not clearly define the loss of TMSiOH, [$^2H_9$]-TMSiOH, and [^{18}O]-TMSiOH, respectively in the formation of m/z 215. This is due to the apparent tendency of the fragment ions to lose additional H_2 neutrals. For example, the unlabeled precursor appears to generate ions corresponding to $[M - TMSiOH]^+$, $[M - TMSiOH - H_2]^+$, and $[M - TMSiOH - 2H_2]^+$ at m/z 215, 213, and 211, respectively. This behavior is not surprising in light of the proposed structure and the possibility for aromatization or extension of conjugation, as shown in Scheme VII. With this apparent tendency in mind, it can be tentatively suggested, using the same arguments as for the m/z 403 ion, that the TMS group originally on the C_3 oxygen becomes bonded to the C_6 oxygen. Because of the obvious labile nature of structure **13**, it is difficult to predict what other decompositions might occur besides the observed loss of TMSiOH and additional H_2 neutrals.

Conclusion

A variation of the TMS group migration first reported by Brooks et al. [10] has been demonstrated. This variation has been found to occur on electron-impact ionization of TMS derivatives of certain 3β-hydroxy

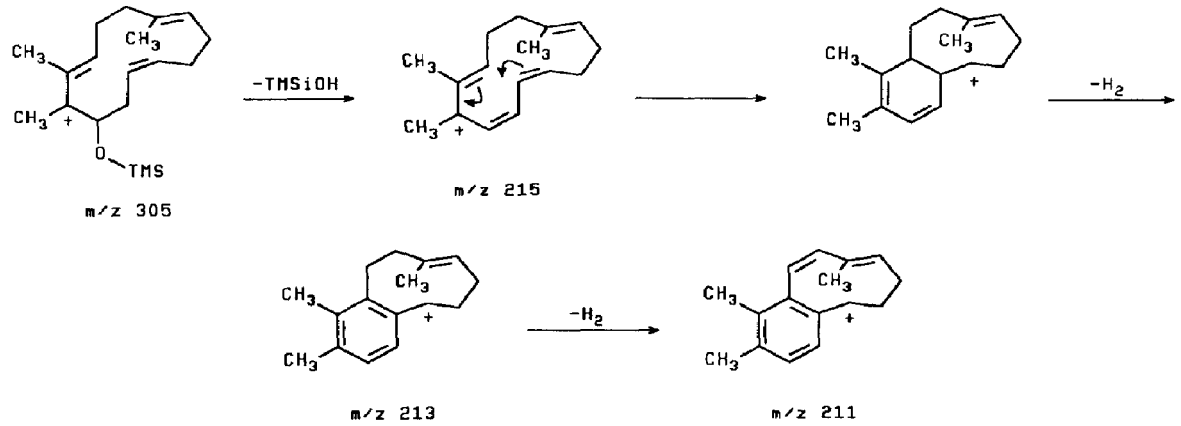

Scheme VII. Conjugation and aromatization of $[M - 56 - 113]^+$ by sequential TMSiOH and H_2 losses.

steroids having oxygenated functionalities, such as epoxide, keto, and hydroxy groups, in various positions on the B ring. Specifically, TMS migration is shown to occur in the presence of an epoxide group at the C_5–C_6 position, a keto group in the C_6 or the C_7 position, and hydroxy groups in the C_5 position. In addition, the position of the target functional group appears to have a greater effect on product structure than the functional group itself. For instance, the CID spectra of m/z 403 produced by **1**, **2**, **6**, and **8** suggest an identical structure with a highly stabilized and delocalized charge center. This is consistent with predictions based on the proposed structure. On the other hand, the CID spectrum of m/z 403 produced by ionic fragmentation of **5**, the only structure with a target functional group at C_7, suggests a structure that is not only different from that produced by **1**, **2**, **6**, and **8**, but is also not as heavily stabilized by extensive charge delocalization. Although the $[M - 71]^+$ ion is small (approximately 10% of the $M^{+\cdot}$ intensity) relative to other common fragments in the electron-impact spectra of trimethylsilylated hydroxy steroids, it may provide important information with regard to the presence of oxygenated functional groups in the C_5, C_6, and C_7 positions of the B ring. In addition, these data further demonstrate the utility of CID in probing features of ion structure.

Acknowledgment

We thank Professor Robert Raffuaf of the College of Pharmacy, Northeastern University, for kindly providing the sample of 5,6β-epoxy-5β-cholestan-3β-ol.

References

1. Vouros, P. In *Practical Spectroscopy Series, Vol. 3, Mass Spectrometry, Part B*; McEwen, C. N., Merrit, C. Jr., Eds.; Marcel Dekker: New York, 1981.
2. Pitt, G. C.; Bursey, M. M.; Chatfield, D. A.; Greenberg, R. S. *J. Organomet. Chem.* **1975**, *90*, 269.
3. Odiorne, T. J.; Harvey, D. J.; Vouros, P. *J. Phys. Chem.* **1972**, *76*, 3217–3220.
4. Clemens, D.; Munson, B. *Org. Mass Spectrom.* **1985**, *20*, 368–373.
5. Orlando, R.; Strobel, F.; Ridge, D. P.; Munson, B. *Org. Mass Spectrom.* **1987**, *22*, 597–605.
6. Orlando, R.; Ridge, D. P.; Munson, B. *Org. Mass Spectrom.* **1988**, *23*, 527–534.
7. Lin, Y.; Ridge, D. P.; Munson, B. *Org. Mass Spectrom.* **1991**, *26*, 550–558.
8. Petersson, G. *Org. Mass Spectrom.* **1972**, *6*, 577.
9. Kingston, D. G. I.; Bursey, J. T.; Bursey, M. M. *Chem. Rev.* **1974**, *2*, 215–242.
10. Brooks, C. J. W.; Harvey, D. J.; Middleditch, B. S. *J. Org. Chem.* **1972**, *37*, 3365.
11. Björkem, I.; Gustafsson, J.-A.; Sjövall, J. *Org. Mass Spectrom.* **1973**, *7*, 277.
12. Gaskell, S.; Smith, A. G.; Brooks, C. J. W. *Biomed. Environ. Mass Spectrom.* **1975**, *2*, 148.
13. Wasilchuk, B. A.; LeQuesne, P. W.; Vouros, P. *Anal. Chem.* **1992**, *64*, 1077–1087.
14. *Lancet* **1980**, May 3, 964–965.
15. Imai, H.; Werthessen, N. T.; Subramanyam, V.; LeQuesne, P. W.; Soloway, A. H.; Kanisawa, M. *Science* **1980**, *207*, 651–653.
16. Diekman, J.; Djerassi, C. *J. Org. Chem.* **1967**, *32*, 1005–1012.
17. Hajdasz, D.; Squires, R. *J. Chem. Soc., Chem. Commun.* **1988**, 1212–1214.